Journal of Structural Geology, Vol. 13, No. 5, pp. 587 to 594, 1991
Printed in Great Britain

0191-8141/91 $03.00+0.00

Volume loss, fluid flow and state of strain in extensional mylonites from the central Mojave Desert, California

ALLEN F. GLAZNER

Department of Geology, CB# 3315, University of North Carolina, Chapel Hill, NC 27599, U.S.A.

and

JOHN M. BARTLEY

Department of Geology and Geophysics, University of Utah, Salt Lake City, UT 84112, U.S.A.

(*Received* 24 *April* 1990; *accepted in revised form* 20 *October* 1990)

Abstract—Compositional changes in mylonitic rocks from the central Mojave metamorphic core complex, California, indicate that large volume loss (20–70%) attended formation of mylonite along the Waterman Hills detachment fault. Strong silica depletion and significant mobility of normally immobile elements imply large fluid/rock ratios during mylonitization, possibly as a result of multiple-pass hydrothermal convection connecting near-surface and mid-crustal alteration regimes. Dissolution of quartz during mylonitization indicates that the fluid was undersaturated with respect to silica, and therefore was probably not magmatic or connate. Large volume loss in a shear zone should result in apparent flattening strains, yet mylonites throughout the complex, including the mylonites that record large volume loss, exhibit constrictional strains. This inconsistency raises questions about the applicability of the shear-zone model to Cordilleran metamorphic core complexes.

INTRODUCTION

GEOCHEMICAL studies of mylonites indicate that mylonitization can cause large changes in bulk-rock chemistry. Commonly reported chemical changes include depletion of Si, K and other mobile elements, enrichments in many immobile elements (e.g. Zr, Ti, P, rare-earth elements), and shifts in stable-isotope ratios. Chemical changes are especially striking in phyllonites (e.g. Drury 1974, Sinha *et al.* 1986, O'Hara 1988, 1990, O'Hara & Blackburn 1989).

In this note we report data which indicate similar bulk-chemical changes during formation of mylonite along a Tertiary low-angle normal fault (the Waterman Hills detachment fault) in the central Mojave Desert. The mass transfer indicated by these data is significant for two reasons. First, it supports the hypothesis that mylonite zones are conduits for large volumes of metamorphic fluids (e.g. Kerrich *et al.* 1984, Sinha *et al.* 1986), as was previously suggested for low-angle normal faults by Kerrich & Rehrig (1987), Reynolds & Lister (1987) and Roddy *et al.* (1988). Second, O'Hara (1988) and Dicken (1988) interpreted immobile-element enrichments during mylonitization along thrust faults to indicate large volume loss. For strain analyses to be accurate, strain measurements must be corrected for effects of volume loss (e.g. O'Hara, 1990). However, fabric relations in the Waterman Hills conflict with the predicted effects of volume loss in a shear zone, raising questions about the applicability of the shear-zone model in this setting.

GEOLOGIC SETTING

Mylonites that form the focus of this study are exposed in the central Mojave metamorphic core complex north of Barstow, California (Fig. 1), in the footwall of the Waterman Hills detachment fault. The geology and regional tectonic setting of the central Mojave metamorphic core complex are discussed in detail elsewhere (Glazner *et al.* 1988, 1989, Bartley *et al.* 1990, Walker *et al.* 1990). The Waterman Hills detachment fault is an Early Miocene low-angle normal fault that emplaced Miocene volcanic and sedimentary rocks upon mylonitized mid-crustal plutonic and metamorphic rocks. At least some of the mylonites formed in the early Miocene during crustal extension (Walker *et al.* 1990). As in other Cordilleran metamorphic core complexes (cf. Davis 1983, Davis *et al.* 1986), footwall structural features, such as downward disappearance of ductile strain and areally consistent shear-sense indicators in the mylonites, suggest that mylonitization occurred in a large-scale normal-sense shear zone. Shear-sense indicators in the central Mojave metamorphic core complex include *S–C* composite fabrics, mica fish, sigma-type quartz augen and dynamically recrystallized quartz grains that are elongate oblique to shear foliation (Bartley *et al.* 1990). Regional tectonics and thermal considerations also support the normal-sense shear zone interpretation of Cordilleran metamorphic core complexes (e.g. Wernicke 1981, Bartley & Wernicke 1984, Buck 1988).

The footwall of the Waterman Hills detachment fault

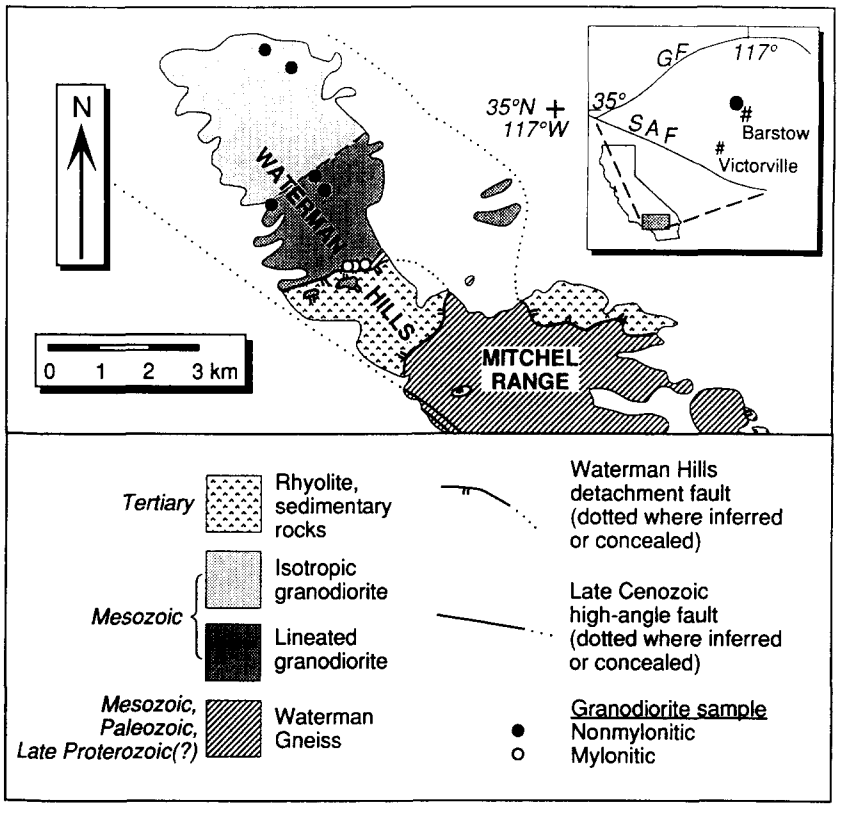

Fig. 1. Location of the Waterman Hills and the central Mojave metamorphic core complex. Sample locations refer to samples averaged in Table 1.

comprises two units. The older of the two is the Waterman Gneiss, a heterogeneous assemblage of metasedimentary and metaigneous rocks of probable Late Proterozoic, Paleozoic and Mesozoic age (Dibblee 1967, Stewart & Poole 1975, Walker *et al.* 1990). The Waterman Gneiss is intruded by a Mesozoic or Tertiary biotite granodiorite pluton that forms the bulk of footwall exposures in the Waterman Hills. The gneiss contains a Mesozoic(?) amphibolite-grade metamorphic fabric that is absent in the granodiorite, but both units were affected by Miocene greenschist-grade mylonitization (Bartley *et al.* 1990). The hanging wall of the detachment fault comprises internally faulted, steeply tilted lava flows, tuffs and clastic sedimentary rocks that have been affected by intense potassium metasomatism. We undertook a geochemical study of hanging-wall and footwall alteration in the Waterman Hills to test models for the genesis of upper-plate potassium metasomatism (Glazner & Bartley 1989, Bartley & Glazner 1990). The present paper focuses on footwall alteration; complete data from the study, which is still in progress, will be reported in a future paper.

The footwall granodiorite is ideal for an alteration study because it is relatively homogeneous and can be traced in outcrop from untectonized rock to strongly lineated ultramylonite (Fig. 2) (Glazner *et al.* 1988, Bartley *et al.* 1990). For convenience, three microstructural types of the granodiorite can be distinguished, but the field relations between these types are entirely gradational. Far from the Waterman Hills detachment fault, the granodiorite is isotropic or possesses a diffuse biotite lineation. The untectonized granodiorite contains quartz (20–30 vol%), plagioclase (40–50 vol%; normally zoned from An_{36} to An_{24}, averaging An_{30}), orthoclase (10–20 vol%), biotite (1–10 vol%), hornblende (0–2 vol%), and traces of apatite, sphene and allanite. The lineation gradually intensifies southward (structurally upward) such that the granodiorite becomes strongly lineated protomylonite within 2 km of the trace of the fault, and mylonite and ultramylonite within 10–20 m of the fault (Fig. 2). Field relations clearly indicate that mylonites formed in response to movement along the detachment fault because mylonite is found only within 10–20 m of the fault contact and this relation persists for nearly 3 km along strike (Bartley *et al.* 1990, fig. 5).

Field and petrographic studies reveal that only one lineation, of consistent character but varying intensity, is present in the granodiorite. This lineation formed in the solid state under greenschist-facies conditions. Microstructures in granodiorite ranging from faintly lineated to mylonitic are typical of granitoids deformed in the greenschist facies near the brittle–ductile transition (see Bartley *et al.* 1990, fig. 7, for photomicrographs): quartz was dynamically recrystallized, feldspar was cracked and replaced by secondary minerals, and biotite underwent basal glide to form kink bands and was altered to chlorite + sphene + magnetite. Quantitative data concerning physical conditions during mylonitization are lacking, but the petrographic relations just described suggest that the temperature was in the range 300–400°C.

Isotropic and protomylonitic granodiorite are cut by numerous steeply dipping cataclastic zones that merge

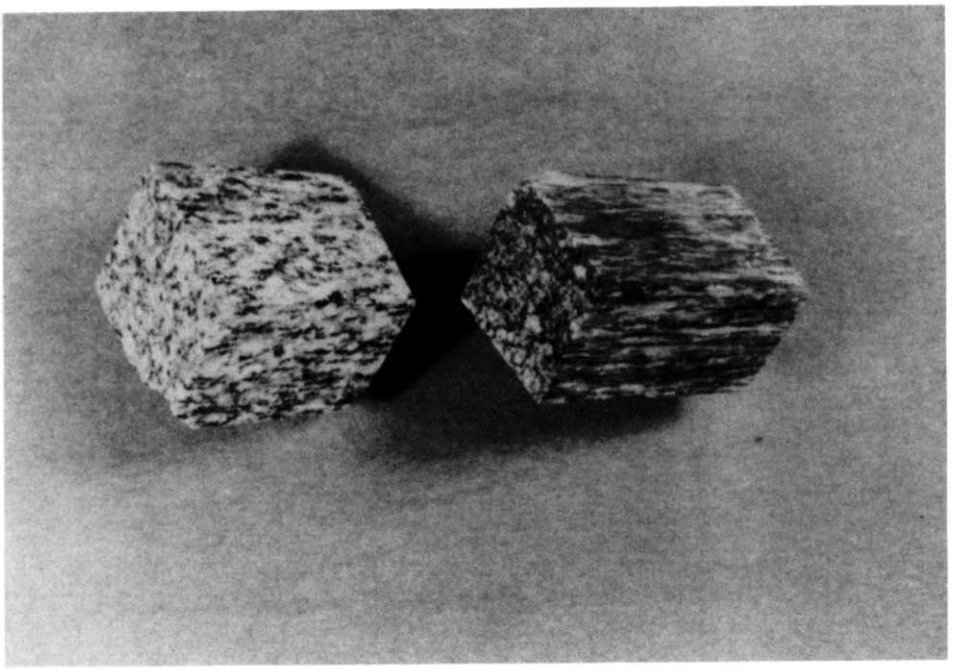

Fig. 2. Sawed blocks of lineated granodiorite, showing progressive development of lineation toward the Waterman Hills detachment fault. Block on left (4 × 3 × 5 cm) is from several hundred meters from the fault and shows a moderate biotite lineation; block on right is from 10 m below fault and shows a strong mylonitic lineation. These blocks are typical in having little or no foliation.

upward into a zone of pervasive distributed cataclasis which overprints the protomylonite and mylonite within several hundred meters of the detachment. In the cataclastic rocks all minerals were deformed by microcracking, with fractures filled by chlorite, quartz, plagioclase and calcite. Based on field relations and structural analysis, Bartley *et al.* (1990) interpreted the cataclastic deformation to record a later, lower-temperature phase of the same crustal extension that formed the mylonites. These zones of highly fractured rock may have played a significant role in synkinematic fluid flow and metasomatism. A connection between fluid flow in the mylonites and that in the cataclastic rocks is corroborated by a similar alteration mineral assemblage having formed in both kinds of tectonite.

EVIDENCE FOR VOLUME LOSS

Volume loss is indicated by large enrichments in many low-mobility elements (e.g. Ti, Zr, P, Cr), coupled with large depletions in mobile elements (e.g. Si, K, Rb). Average analyses of fresh granodiorite and its ultramylonitic equivalent are given in Table 1. Typical relationships between SiO_2 depletion and enrichments of low-mobility elements are shown in Fig. 3. Low-mobility elements are anticorrelated with SiO_2 and are typically enriched by factors of 2–6 in ultramylonite.

Figure 4 shows element concentration changes for all elements that have been analysed. Density changes during alteration are minor (Table 1). Interpretation of these concentration changes is non-unique unless either the volume change or the absolute gain or loss of an element can be determined independently (Gresens 1967), which is impossible in the present case. The pattern could be interpreted to reflect constant-volume alteration, with elements on the left side of the diagram removed from the mylonite and elements on the right side added. However, following O'Hara (1988) we instead interpret the pattern to indicate large volume loss caused by loss of elements on the left side of the diagram (in particular, Si), resulting in residual enrichment of those on the right side. This interpretation is supported by the fact that many elements that are enriched in the mylonite commonly are immobile in hydrothermal systems (e.g. Ti, Zr, P, Hf and light rare-earth elements), whereas elements that are depleted in the mylonite are known to be highly mobile in hydrothermal systems (e.g. K, Rb and Si). Glazner & Bartley (1989) showed that the footwall depletions are generally complementary to hanging-wall enrichments; for example, upper-plate rocks are silicified and highly enriched in K and Rb.

Dissolution of primary quartz probably contributed to the loss of Si, but this is difficult to assess quantitatively because fine grain size and complex micron-scale mineral intergrowths in the mylonites make it impossible to determine accurate modes. However, study of the mylonites with the optical microscope and electron microprobe reveals that feldspar breakdown reactions

Table 1. Comparison of granodiorite and mylonite compositions

	Major elements			Trace elements	
	granodiorite	mylonite		granodiorite	mylonite
n	5	3	*n*	3	3
SiO_2	68.3 ± 3.8	54.9 ± 2.4	Sb	0.13 ± 0.06	1.03 ± 0.32
TiO_2	0.38 ± 0.23	1.19 ± 0.20	Co	4.47 ± 1.6	13.7 ± 1.2
Al_2O_3	14.8 ± 0.51	16.9 ± 0.14	Zr	79.5 ± 47	240 ± 66
FeO^t*	2.39 ± 1.0	7.20 ± 1.2	Sc	4.78 ± 1.0	12.0 ± 0.96
MgO	0.90 ± 0.41	3.65 ± 0.25	Cr	8.27 ± 2.4	20 ± 3.0
CaO	2.73 ± 0.77	4.08 ± 1.0	Eu	0.94 ± 0.21	1.85 ± 0.30
Na_2O	4.09 ± 0.58	3.90 ± 0.11	Hf	3.5 ± 0.75	6.2 ± 1.0
K_2O	3.01 ± 0.98	1.62 ± 0.17	Zn	30 ± 0	50 ± 10
P_2O_5	0.31 ± 0.15	0.80 ± 0.08	Nd	15.3 ± 1.5	22.0 ± 6.1
LOI	2.16 ± 2.3	4.47 ± 0.31	Sm	3.01 ± 0.17	4.22 ± 1.2
Total	99.2	98.7	Sr	400 ± 100	533 ± 208
			Ce	36.3 ± 4.2	48.0 ± 15
			La	21.2 ± 3.5	27.9 ± 9.9
ρ†	2.61 ± 0.01	2.69 ± 0.04	Tb	0.4 ± 0	0.5 ± 0.17
			Br	2.20 ± 0.79	2.57 ± 0.49
			Ba	743 ± 71	670 ± 221
			Yb	1.41 ± 0.13	1.27 ± 0.20
			U	2.1 ± 0.17	1.8 ± 0.6
			Lu	0.21 ± 0.02	0.18 ± 0.02
			Rb	96.7 ± 25	60.0 ± 17
			Th	6.93 ± 0.21	4.03 ± 2.0
			Cs	3.97 ± 2.8	0.87 ± 0.06

Major elements in wt%; analysed by X-ray fluorescence on glass and pressed-powder disks and by atomic absorption spectroscopy (for Na and Mg). Trace elements analysed by commercial instrumental neutron activation analysis. Trace elements ranked by increasing enrichment factor in mylonites. *n* = number of samples averaged. Value after "±" indicates standard deviation of averaged values.

*FeO^t indicates total Fe calculated as FeO.

†ρ = density in g cm^{-3}, determined by Jolly balance.

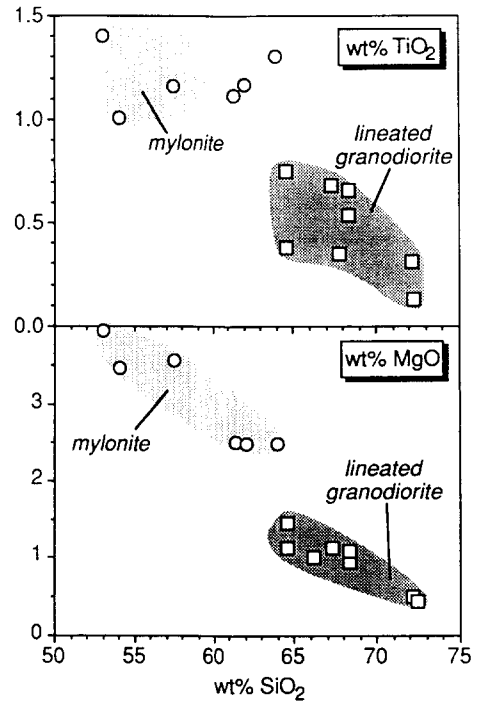

Fig. 3. Typical anticorrelation of immobile elements with silica. Enrichments in relatively immobile elements such as Ti, Mg and Zr are interpreted to be a result of extreme volume loss caused in large part by leaching of silica. Figure includes data from Table 1 as well as partial analyses from other samples.

during mylonitization of the granodiorite account for at least part of the K, Rb and Si losses. Rather than being hydrolysed to form phyllosilicates (e.g. O'Hara 1988, 1990), plagioclase and orthoclase both were replaced by An_{38} plagioclase, that is, plagioclase more calcic than that in the protolith (Bartley & Glazner 1990). If written conserving Al, the replacement reactions liberate silica as well as most of the K and Rb in the protolith. If Al actually was lost from the protolith during mylonitization (see below), the amount of silica liberated from feldspar increases accordingly.

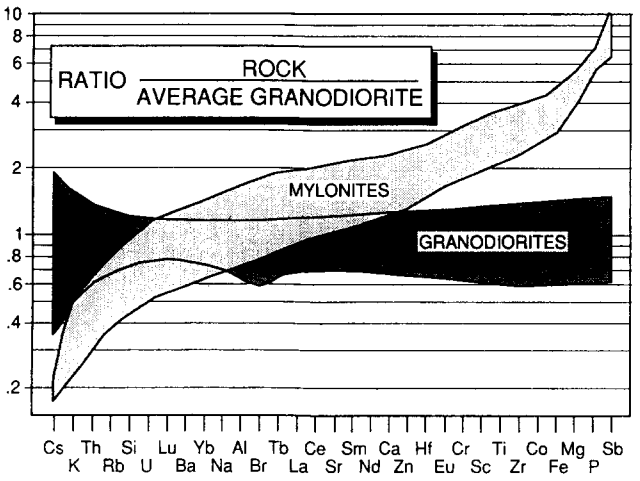

Fig. 4. Relative elemental enrichments and depletions during conversion of granodiorite to mylonite. Each band encompasses three analyses. Elements ranked by increasing enrichment in mylonite. Logarithmic ordinate plots the ratio of the concentration of an element in the mylonite to the concentration of that element in the average of three granodiorites (Table 1). Note that relatively mobile elements (e.g. K, Rb, Si) are depleted in mylonite, and relatively immobile elements (e.g. Zr, Mg, Ti) are concentrated in mylonite.

If the elements on the right side of Fig. 4 were truly immobile and the mean of analyses of the granodiorite protolith were representative, then all of the immobile elements in a given analysis should show a constant enrichment factor. Instead, the enrichments shown by the mylonites are quite variable, indicating one or more of the following: (1) the unaltered granodiorite is not representative of the mylonite protolith; (2) primary compositional variation in the protolith was incompletely averaged out with the samples analysed; and (3) low-mobility elements show differential mobility, possibly including both net additions and subtractions. The clear gradation observed in the field from granodiorite to mylonite indicates that the first possibility is not a serious problem. Additional analyses (in progress) will help to address the second possibility, but we believe that this will prove to be a second-order source of scatter. Thus, we infer that the variable enrichments of low-mobility elements reflect differential mobility.

The relatively gently sloping center of the sigmoidal pattern of enrichments in Fig. 4 corresponds to elements with similar enrichments in the range from about 1.5 to 3. This interval includes virtually all of the high field-strength minor and trace elements that are widely assumed to be immobile in hydrothermal alteration. Ti, Zr, Co and Fe lie at the upper end of this gently sloping interval, with average enrichments of 2.75–3.2 (Table 1). Enrichment factors beyond Fe define a steep tail of extreme and variable enrichments from 4.5 to 8.

We infer that true immobility was most closely approached by the elements with enrichment factors around 3. When coupled with the modest density change that accompanied alteration (Table 1), this implies that the typical volume loss was of the order of 60–70 vol%. Elements that define the gentle slope to the left of Ti, Zr, Co and Fe in Fig. 4 (e.g. rare-earth elements) were relatively immobile but suffered variable amounts of leaching during alteration. Among such leached elements is Al, the concentration of which changed only slightly during alteration. Because of its low solubility in aqueous fluids, Al commonly is assumed to be immobile during rock alteration (cf. Kerrick 1988). Aluminum mobility appears to be inescapable in this case, however, because the alternative, addition of elements that plot to the right of Al in Fig. 4 in amounts proportional to their enrichment factors, seems far less probable. However, the enrichment factors of Mg, P and Sb are so extreme and different from other elements that it seems likely that these elements did undergo net additions from the hydrothermal fluid.

IMPLICATIONS

Fluid flow

The silica depletion implied by the data in Table 1 indicates that large volumes of fluid have passed through

the mylonite zone in the Waterman Hills. A minimal estimate of the fluid/rock volume ratio can be made given an estimate of silica solubility in the fluid and assuming that (1) there initially was no silica in the fluid and (2) some element was immobile. Using the silica solubility equation of Fournier & Potter (1982) and assuming Ti was perfectly immobile, O'Hara & Blackburn (1989) estimated minimum fluid/rock weight ratios of 70–600 for phyllonitization of granitic gneisses in the Blue Ridge of Virginia and North Carolina. The same calculation using data from Table 1 and temperatures of 300 and 400°C gives fluid/rock ratios of 500 and 160, respectively. Such large fluid/rock ratios are corroborated qualitatively by the substantial differential enrichment just noted of normally immobile elements such as Al and rare earths, which could be achieved most readily by variable leaching of slightly soluble elements by a very large volume of fluid.

Large fluid/rock ratios imply that the mylonite zone served as a fluid channel. Two end-member geological scenarios for fluid movement along the mylonite zone could be considered: a single upward pass of magmatic or metamorphic fluid with extreme focusing of flow, as favored by Reynolds & Lister (1987) for the South Mountains metamorphic core complex of Arizona, or multiple fluid passes by large-scale convection, which we favor for the Waterman Hills area. Three lines of evidence support multiple-pass convection in the Waterman Hills. First, bulk chemical and mineralogical changes resulting from upper-plate and lower-plate alteration are complementary (Glazner & Bartley 1989, Bartley & Glazner 1990). Second, intense alteration and mineralization along the deeply penetrating cataclastic zones that cut the mylonite (Glazner & Bartley 1989, Bartley *et al.* 1990) suggest that these cataclastic zones may be part of the recharge system required for large-scale fluid convection. Third, the observed leaching of silica during lower-plate alteration requires that the fluid entering the lower-plate rock was undersaturated with respect to silica. It is difficult to envisage how magmatic or connate fluids could be silica-undersaturated, especially because such a fluid would be moving down the temperature gradient. However, cool near-surface water convectively recycled into the lower plate would become highly silica-undersaturated as a result of increases in both temperature and pressure, and therefore could be expected to dissolve silica from its surroundings.

Structural analysis

Strain compatibility arguments predict plane strains in an ideal shear zone, and that any volume changes should be accommodated by contraction or dilation in a direction perpendicular to the shear zone walls (Ramsay & Graham 1970). A combination of plane strain and volume loss therefore should result in apparent flattening strains (e.g. Ramsay & Wood 1973). This prediction received observational support from O'Hara (1990), who found mildly to strongly oblate grain-shape fabrics in Appalachian thrust-related mylonites that show geochemical evidence for large volume loss. Because uniaxial volume loss will exaggerate rotations of markers in a shear zone, the probable result will be an overestimate of shear strains. Theory suggests that measured shear strains might be corrected for a known volume loss by redilating the shear zone along its normal by the appropriate amount, although in practice this procedure could be complicated by heterogeneous strains (O'Hara 1990).

However, fabric relations indicate that this theory is inappropriate to the Waterman Hills, and therefore we are uncertain how strain data from these rocks could be corrected for volume loss. The intense mylonitic lineation in the granodiorite only rarely is developed within an associated foliation, and such a foliation where present commonly is so weak that it cannot be measured confidently in the field (Fig. 2) (Glazner *et al.* 1988, Bartley *et al.* 1990). A purely *L*-tectonite fabric ordinarily is taken to record constrictional finite strain. Magnetic susceptibility anisotropy measurements and analysis of the orientation and styles of folds in the Waterman Gneiss suggest that constrictional strains predominate throughout the central Mojave core complex (Fletcher & Bartley 1990, and manuscript in preparation).

We presently cannot explain this combination of volume loss and constrictional strain. It is unclear how uniformly constrictional strains can be achieved in a shear zone, because most expected deviations from plane strain in a shear zone (e.g. strain gradients and propagation effects) lead to flattening, not constriction (e.g. Coward 1976). Large volume loss in the mylonites exacerbates the problem because even these rocks lack a foliation. Two possibilities might be considered: the rock fabrics might not accurately record the finite strain field, or the macroscopic structural geometry could deviate greatly from the shear-zone model. Microstructures in tectonites of the central Mojave metamorphic core complex (Bartley *et al.* 1990) are typical of shear-zone rocks elsewhere that have yielded reasonable strain data, and therefore we doubt that the rocks provide such a poor record of finite strain. The alternative is that the shear-zone model is inappropriate for the central Mojave metamorphic core complex and therefore it cannot explain the strain field. While the major successes of the shear-zone model make it likely that its most essential feature, concentrated non-coaxial strain in the middle crust, is generally accurate, strain analysis based on assumption of an ideal shear-zone geometry may be inappropriate in this setting.

CONCLUSIONS

Bulk-rock geochemistry of mylonites in a major extensional shear zone exposed in the Waterman Hills implies that their formation involved large (up to 70%) volume loss and large fluid/rock ratios. Because alteration and volume loss accompanied mylonite formation, the fluid/rock ratios may reflect synextensional fluids

involving the upper and middle crust. The mylonites, like mylonitic rocks throughout the metamorphic core complex, appear to record constrictional strain rather than the strong apparent flattening expected from large volume loss in a shear zone. The large-scale kinematic framework for the constrictional strain is yet poorly understood, but it probably deviates substantially from the ideal shear-zone model.

Acknowledgements—We thank Kieran O'Hara and an anonymous reviewer for constructive reviews of the manuscript, John M. Fletcher for allowing us to cite his unpublished strain data on mylonites from the Waterman Gneiss, and Sydney B. Dent and Stefan S. Boettcher for help with field work and sample collection. Supported by National Science Foundation grants EAR-8817071 to A. F. Glazner and EAR-8816944 to J. M. Bartley.

REFERENCES

Bartley, J. M., Fletcher, J. M. & Glazner, A. F. 1990. Tertiary extension and contraction of lower-plate rocks in the central Mojave metamorphic core complex, southern California. *Tectonics* **9**, 521–534.

Bartley, J. M. & Glazner, A. F. 1990. Petrological evidence of large-scale pore fluid convection in the central Mojave metamorphic core complex, California. *Eos* **65**, 1663.

Bartley, J. M. & Wernicke, B. P. 1984. The Snake Range décollement interpreted as a major extensional shear zone. *Tectonics* **3**, 647–657.

Buck, W. R. 1988. Flexural rotation of normal faults. *Tectonics* **7**, 959–973.

Coward, M. P. 1976. Strain within ductile shear zones. *Tectonophysics* **34**, 181–197.

Davis, G. A., Lister, G. S. & Reynolds, S. J., 1986. Structural evolution of the Whipple and South Mountains shear zones, southwestern United States. *Geology* **14**, 7–10.

Davis, G. H. 1983. Shear-zone model for the origin of metamorphic core complexes. *Geology* **11**, 342–347.

Dibblee, T. W., Jr. 1967. Areal geology of the western Mojave Desert, California. *Prof. Pap. U.S. geol. Surv.* **522**.

Dicken, A. P. 1988. Evidence for limited REE leaching from the Roffina Gneiss, Switzerland—A discussion of the paper by Vocke *et al.* (1987) (*Contr. Miner. Petrol.* **95**, 145–154). *Contr. Miner. Petrol.* **99**, 273–275.

Drury, S. A. 1974. Chemical changes during retrogressive metamorphism of Lewisian granulite facies rocks from Coll and Tiree. *Scott. J. Geol.* **10**, 237–256.

Fletcher, J. M. & Bartley, J. M. 1990. Constrictional strain in the footwall of the central Mojave metamorphic core complex, California. *Geol. Soc. Am. Abs. w. Prog.* **22**, 23.

Fournier, R. O. & Potter, R. W., 1982. An equation correlating the solubility of quartz in water from 25 to 900°C at pressures up to 10,000 bars. *Geochim. cosmochim. Acta* **46**, 1969–1973.

Glazner, A. F. & Bartley, J. M. 1989. Source of potassium in potassium-metasomatized, extended Tertiary rocks of the Mojave Desert. *New Mexico Bur. Mines Min. Res. Bull.* **131**, 109.

Glazner, A. F., Bartley, J. M. & Walker, J. D. 1988. Geology of the Waterman Hills detachment fault, central Mojave Desert, California. In: *This Extended Land—Geological Journeys in the Southern Basin and Range,* (edited by by Weide, D. L. & Faber, M. L.). *Spec. Publ. Univ. Nevada, Las Vegas* **2**, 225–237.

Glazner, A. F., Bartley, J. M. & Walker, J. D. 1989. Magnitude and significance of Miocene crustal extension in the central Mojave Desert, California. *Geology* **17**, 50–53.

Gresens, R. L. 1967. Composition-volume relationships of metasomatism. *Chem. Geol.* **2**, 47–65.

Kerrick, D. M. 1988. Al_2SiO_5-bearing segregations in the Lepontine Alps, Switzerland: Aluminum mobility in pelites. *Geology* **16**, 636–640.

Kerrich, R., La Tour, T. E. & Wilmore, L. 1984. Fluid participation in deep fault zones: evidence from geological, geochemical and $^{18}O/^{16}O$ relations. *J. geophys. Res.* **89**, 4331–4343.

Kerrich, R & Rehrig, W. 1987. Fluid motions associated with Tertiary mylonitization and detachment faulting: $^{18}O/^{16}O$ evidence from the Picacho metamorphic core complex, Arizona. *Geology* **15**, 58–62.

O'Hara, K. 1988. Fluid flow and volume loss during mylonitization: An origin for phyllonite in an overthrust setting, North Carolina, U.S.A. *Tectonophysics* **156**, 21–36.

O'Hara, K. 1990. State of strain in mylonites from the western Blue Ridge province, southern Appalachians: The role of volume loss. *J. Struct. Geol.* **12**, 419–430.

O'Hara, K. & Blackburn, W. H. 1989. Volume-loss model for trace element enrichments in mylonites. *Geology* **17**, 524–527.

Ramsay, J. G. & Graham, R. H. 1970. Strain variations in shear belts. *Can. J. Earth Sci.* **7**, 786–813.

Ramsay, J. G. & Wood, D. S. 1973. The geometric effects of volume change during deformational processes. *Tectonophysics* **16**, 263–277.

Reynolds, S. J. & Lister, G. S. 1987. Structural aspects of fluid-rock interactions in detachment zones. *Geology* **15**, 362–366.

Roddy, M. S., Reynolds, S. J., Smith, B. M. & Ruiz, J. 1988. K-metasomatism and detachment-related mineralization, Harcuvar Mountains, Arizona. *Bull. geol. Soc. Am.* **100**, 1627–1639.

Sinha, A. K., Hewitt, D. A. & Rimstidt, J. D. 1986. Fluid interaction and element mobility in the development of ultramylonites. *Geology* **14**, 833–886.

Stewart, J. H. & Poole, F. G., 1975, Extension of the Cordilleran miogeosynclinal belt to the San Andreas fault, southern California. *Bull. geol. Soc. Am.* **86**, 205–212.

Walker, J. D., Bartley, J. M. & Glazner, A. F. 1990. Large-magnitude Miocene extension in the central Mojave Desert: Implications for Paleozoic to Tertiary paleogeography and tectonics. *J. geophys. Res.* **95**, 557–569.

Wernicke, B. P. 1981. Low-angle normal faults in the Basin and Range province: Nappe tectonics in extending orogen. *Nature* **291**, 645–648.